

Study of Phantom Images with Silicone Rubber on Single Photon Emission Computed Tomography (SPECT)

Zaenal Arifin^{1*}, Heri Sutanto¹, Siti Fairus², Anis Suhana³

¹Department of Physics, Faculty of Science and Mathematics, Diponegoro University, Jl. Prof. Soedarto SH, Tembalang, Semarang, Central Java, Indonesia

²Physics, University Malaya, Malaysia

³Pusat Perubatan University Malaya, Malaysia

*Corresponding author : zaenalarifin@fisika.fsm.undip.ac.id

ARTICLE INFO

Article History:

Accepted: 05 Jan 2024

Published: 18 Jan 2024

Publication Issue :

Volume 11, Issue 1

January-February-2024

Page Number :

167-172

ABSTRACT

Silicon rubber has been used as a protective material to shield sensitive organs of patients located near the skin surface during CT scan examinations. However, the quality of the resulting images has not been thoroughly investigated. This study was to evaluate the resulting image quality of a new synthetic thyroid shield based on silicon rubber (SR)-lead (Pb) composites thyroid shields in single photon emission computed tomography (SPECT) examination of the neck phantom. The synthetic SR-Pb thyroid shield had a Pb percentage from 0 to 5 wt% and a thickness of 0.6 cm. Scanning on the neck phantom was performed with and without the SR-Pb. The thyroid shields were placed directly on the neck surface. Image quality was characterized by spatial resolution on the areas of anterior, posterior and lateral of the neck phantom. Detailed evaluation of the image quality was employed by image subtraction. The SR-Pb shield produced only a very small artefact, increasing spatial resolution in the posterior area by only 9%. The SR-Pb shield is suitable in the daily clinical setting for thyroid in SPECT examinations while maintaining image quality.

Keywords: Phantom Image, SR-Pb Thyroid Shield, TC-99m, SPECT Uniformity

I. INTRODUCTION

Thyroid examinations conducted at a nuclear medicine facility utilizing radioactive Tc-99m play a pivotal role in diagnosing complaints related to

hypothyroidism or hyperthyroidism among patients [1], [2]. This diagnostic procedure typically involves the use of Single Photon Emission Computed Tomography (SPECT) or a gamma camera, both of

which provide detailed images for a comprehensive assessment of thyroid function [3], [4].

In this procedure, a specific amount of radioactive Tc-99m, usually ranging from 1 to 5 millicuries (mCi), is administered based on the individual patient's needs. The radioactive Tc-99m emits gamma rays with an energy of 140 kilo electron volts (keV). The utilization of SPECT allows for the detection of Tc-99m, and the scanning time typically ranges from 1 to 3 minutes, depending on the examination protocol [5]. To enhance safety during medical imaging, advancements have been made in the development of protective materials [6]. For instance, a silicon rubber with lead (SR-Pb) composite has been engineered to safeguard specific organs, including the thyroid and abdomen, when subjected to CT scans employing X-ray emitters [7]. Research involving SR-Pb composites, ranging from 0% to 5% lead concentration with a thickness of 0.6 mm, has demonstrated a notable reduction in radiation dose of up to 34%, while maintaining clear image quality and minimizing artifacts [8], [9].

While the protective application of SR-Pb composites in X-ray examinations has been extensively studied, its potential application in mitigating gamma ray exposure during nuclear medicine procedures remains unexplored. Therefore, further research is imperative to investigate the efficacy of SR-Pb composites in the context of nuclear medicine examinations, specifically those targeting the thyroid. This research may involve the use of phantoms, including neck phantoms and bar phantoms, to simulate and assess the impact of SR-Pb on radiation exposure and image quality in a controlled environment.

II. METHODS AND MATERIAL

SR-Pb shields and breast phantoms were developed. The SR-Pb shields were tested on the in-house breast phantom positioned above the anthropomorphic phantom. Dose and image quality with and without SR-Pb shields were measured. Furthermore, the SR-

Pb shields were evaluated for its elasticity by mechanical test.

A. Tools and Materials

In the experimental setup, a range of tools and materials were carefully selected to facilitate the comprehensive investigation of nuclear medicine procedures. The application of Tc-99m, varying from 1 to 5 millicuries (mCi), served as the radioactive tracer to simulate real-world conditions in diagnostic imaging. This carefully measured range allowed researchers to explore the optimal dosage for various imaging scenarios.

To replicate the anatomical complexities encountered in medical imaging, specialized phantoms were employed, such as the Jaszczak Phantom. This phantom provided a controlled environment for the study, allowing for the assessment of imaging techniques with a focus on accuracy and reliability [10]. The use of syringes and Phantom Bars was instrumental in the precise administration and preparation of the Tc-99m, ensuring consistency in the experimental conditions. All these tools can be seen on Figure 1.

The introduction of SPECT into the investigative toolkit enhanced the depth and precision of diagnostic imaging. This imaging modality played a pivotal role in capturing three-dimensional images, contributing valuable data to the overall analysis of the experimental results.

In the pursuit of safety and radiation protection, the study explored the use of silicon rubber with lead (SR-Pb) in concentrations ranging from 0 to 5%. This innovative composite material aimed to shield specific organs during imaging procedures, potentially reducing radiation exposure without compromising image quality. Additionally, the incorporation of lead aprons, Ring Thermoluminescent Dosimeters (TLD), and Digital Dose Monitoring underscored the commitment to ensuring the safety of healthcare

practitioners involved in nuclear medicine experiments. We also used Survey meter LUDLUM Model 14C/44-7 SN: 201376/PR208441 to measure the dose.



(a)



(b)



(c)

Figure 1. The images of (a) Jaszczak Phantom, (b) Syringe, and (c) Bar Phantom

B. Experimental Procedure

In the research process, several distinct steps are undertaken to investigate the application of Tc-99m in nuclear medicine examinations. The initial phase involves the meticulous preparation of Tc-99m material to ensure its suitability for the subsequent imaging procedures. Following this, a phantom is prepared, offering various options such as a neck

phantom, bar phantom, or syringe, to simulate real-world conditions during the imaging studies.

Once the phantom is ready, the Tc-99m is carefully charged to Jaszczak phantom or syringe as part of the experimental setup. Specimen preparation follows, ensuring that the conditions closely mimic those encountered in actual medical scenarios. The prepared phantom object containing Tc-99m is then strategically placed in the imaging apparatus to initiate the scanning process.

The research then delves into two distinct scanning scenarios. Firstly, scanning is conducted without the application of silicon rubber-Pb, encompassing activities ranging from 1 to 5 mCi. The scanning time is maintained at 1-3 minutes for each activity (1, 2, 3, 4, and 5). Subsequently, the same scanning activities are repeated, but this time with the inclusion of silicon rubber-Pb. The scanning duration remains consistent at 1-3 minutes for each activity.

The final step involves the critical evaluation of the image results obtained from the phantom or syringe for activities spanning 1 to 5 mCi. This comprehensive assessment includes a comparative analysis of images obtained both with and without the application of silicon rubber-Pb, providing insights into the potential impact of this protective material on image quality and radiation exposure in nuclear medicine examinations.

In this research, the image uniformity values of the phantom with SR-Pb are compared to those without SR-Pb. SPECT uniformity is evaluated both intrinsically (without a collimator) and extrinsically (with a collimator). Intrinsically, a point source (volume < 1 mL, containing ~18.5 MBq) of Tc-99m is placed 5 crystal dimensions above the detector without a collimator to generate nearly uniform photon flux on the detector. Extrinsically, a flood field source (usually 185–555 MBq) of Co-57 is placed directly on the detector with a collimator (Zanzonico,

2009). The uniformity value (IU) is calculated using the following equation:

$$IU [\%] = 100 \frac{C_{\max} - C_{\min}}{C_{\max} + C_{\min}} \quad (1)$$

C_{\max} is the highest count value on the detector, and C_{\min} is the lowest count value on the detector.

In this study, the impact of SR-Pb administration on image quality is analyzed using the Jaszczak phantom. The phantom consists of three sections: rod section, sphere section, and uniformity section (Hirtl et al., 2017). The rod section comprises a set of rod-like structures with varying sizes: 12.7, 11.1, 9.5, 7.9, 6.4, 4.8 mm, while the sphere section consists of spherical structures with varying sizes: 31.8, 25.4, 19.1, 15.9, 12.7, 9.5 mm.

The Jaszczak phantom is filled with water and then administered Tc-99m radioisotopes with an activity of 29 mCi. The phantom is shaken several times to distribute the radioisotopes homogeneously. Placed on the patient bed, the phantom is scanned with a gamma camera. In the scan with SR-Pb, SR-Pb is placed on the phantom's surface, followed by a gamma camera scan. In this image quality test, the resolution is considered good if the smallest sphere structure is detectable (Genç et al., 2019).

III. RESULTS AND DISCUSSION

The initial activity of the Tc-99m source was 29.0 mCi at 25/7/2023, 14:23 p.m. Subsequent measurements at different times indicate a decrease in activity, which is expected as radioactive materials decay over time. The measurements are taken under various shielding conditions denoted by SR-Pb X%, where X represents the percentage of lead used in shielding. The uniformity percentage provides information about the distribution of radioactivity across the source. This data is crucial for monitoring the decay of the Tc-99m source over time and understanding the impact of different lead shielding percentages on its activity and uniformity. It helps ensure safety and proper handling

of radioactive materials in medical or industrial settings.

According to Table 1, the uniformity values show an improvement with the addition of SR-Pb, except when using SR-Pb 3%. In imaging without SR-Pb, a relatively high uniformity value is observed. As a reference, as per IAEA (2003), the following are the limits for SPECT image uniformity:

Table 1. The decay of the Tc-99m source over time

Activity number	Activity Time (p.m.)	Activity (mCi)	Uniformity (%)	Description
1	15:02	26,9	10,82	Material Non-SR
2	15:32	25,4	12,74	SR-Pb 1% (A)
3	15:49	24,6	13,33	SR-Pb 2% (B)
4	16:04	23,9	10,21	SR-Pb 3% (C)
5	16:16	23,3	14,01	SR-Pb 4% (D)
6	16:28	22,8	11,90	SR-Pb 5% (E)

Higher uniformity percentages indicate poorer image quality. Therefore, it is evident that the use of SR-Pb diminishes the image quality of the phantom.

Table 2. Reference Values for SPECT Uniformity

Intrinsic Uniformity		Extrinsic Uniformity	
IU (%)	Description	IU (%)	Description
< 3.5%	Good, no corrective action needed	< 5%	Good, no corrective action needed
3.5–5%	Good, requires corrective action	5–6%	Good, requires corrective action
>5%	Not good, requires corrective action	>6%	Not good, requires corrective action

Figure 1 depicts the scanned image results of the Jaszczak Phantom. Based on figures 2(a-c), it is visually evident that the use of SR-Pb leads to the appearance of distributed noise in the phantom image relative to the image without SR-Pb. This explains the

decrease in image uniformity, as reflected in the increased uniformity values in Table 2.

Figures 2(b) and 2(c) summarize the phantom images in the sphere and rod sections. In Figure 2(b), the 9.5 mm sphere is not clearly visible in both the phantom images without SR-Pb and with SR-Pb. The influence of adding SR-Pb is limited to a reduction in image sharpness. In Figure 2(c), there is a reduction in image quality due to the emergence of noise, causing the rod structure to appear less sharp in the image without SR-Pb. This lack of sharpness makes adjacent rod structures seem merged, ultimately reducing the spatial resolution of the image.

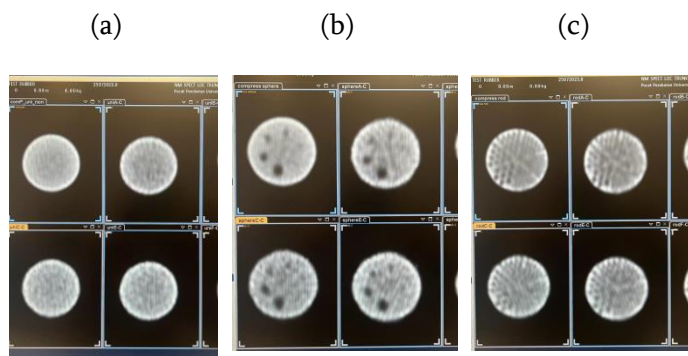


Figure 2. The image of the Jaszczak Phantom after shielded by SR-Pb with various composition, where SR-Pb 1% (A), SR-Pb 2% (B), SR-Pb 3% (C), SR-Pb 4% (D), and SR-Pb 5% (E).

Table 3. provides a comparison of radioactivity levels and exposure rates for different shielding conditions involving Technetium-99m (Tc-99m) and Iodine-131 (I-131). Shielding with lead (SR-Pb) at various percentages (1% to 5%) and using a lead apron (Apron Pb 0.35mm) significantly reduces the exposure rates compared to non-shielded conditions. The exposure rates vary depending on the type of radioactive material and the level of lead shielding applied. It is evident that higher percentages of lead in shielding generally result in lower exposure rates.

Table 3. Measurement of radiation exposure to I-131 iodine and Tc-99m at a distance of 30 cm.

Radioactive	TC-99m	I-131
Activity (mCi)	22,7	9,74
No SR	10 mR/h	30 mR/h
SR-Pb 1% (B)	10 mR/h	30 mR/h
SR-Pb 2% (C)	10 mR/h	30 mR/h
SR-Pb 3% (D)	10 mR/h	20 mR/h
SR-Pb 4% (E)	9 mR/h	20 mR/h
SR-Pb 5% (F)	9 mR/h	20 mR/h
Apron Pb 0.35mm	4 mR/h	0 mR/h

Table 3 summarizes the gamma emission values from Tc-99m and I-131 measured at a distance of 30 cm. According to table 2, it is evident that sr-pb 5% can attenuate a higher fraction of gamma emissions compared to sr-pb with lead concentrations of 1–4%. Intuitively, this can be explained by the effective interaction between gamma rays and lead atoms, which is proportional to the lead concentration in silicon rubber.

IV.CONCLUSION

The image results with all variations of silicone rubber on the Jaszczak phantom with a technetium-99m source were subjectively unclear. This could potentially diminish the analysis of each object within the phantom. In addition, the dose read after the addition of silicon rubber does not have a significant dose reduction effect when compared to the addition of Pb apron. This is due to the small amount of Pb in the silicon rubber mixture.

Acknowledgments

Thank for supporting research form World Class University Program Diponegoro University 2023.

V. REFERENCES

[1]. A. B. A. Ahmed, "Evaluation of Thyroid Abnormalities using Ultrasonography and

- Radionuclide Scintigraphy.” Sudan University of Science and Technology, 2018.
- [2]. H. S. W. Mohammed, “Study of Normal Thyroid Uptake using Technisium-99m.” Sudan University of Science and Technology, 2017.
- [3]. D. Brandon, A. Alazraki, R. K. Halkar, and N. P. Alazraki, “The Role of Single-Photon Emission Computed Tomography and SPECT/Computed Tomography in Oncologic Imaging,” *Semin. Oncol.*, vol. 38, no. 1, pp. 87–108, 2011, doi: <https://doi.org/10.1053/j.seminoncol.2010.11.003>.
- [4]. W. W. Lee and K.-S. Group, “Clinical applications of technetium-99m quantitative single-photon emission computed tomography/computed tomography,” *Nucl. Med. Mol. Imaging (2010)*, vol. 53, no. 3, pp. 172–181, 2019.
- [5]. M. A. Elmakki, “Estimation of Pediatric Patient’s Radiation Dose During Nuclear Medicine Test.” Sudan University of Science and Technology, 2021.
- [6]. M. Prasad et al., “Nanotherapeutics: An insight into healthcare and multi-dimensional applications in medical sector of the modern world,” *Biomed. Pharmacother.*, vol. 97, pp. 1521–1537, 2018.
- [7]. S. Y. Astuti, H. Sutanto, E. Hidayanto, G. W. Jaya, A. S. Supratman, and G. P. Saraswati, “Characteristics of Bolus Using Silicone Rubber with Silica Composites for Electron Beam Radiotherapy,” *J. Phys. Its Appl.*, vol. 1, no. 1, pp. 24–27, 2018.
- [8]. Y. Irdawati, H. Sutanto, C. Anam, T. Fujibuchi, F. Zahroh, and G. Dougherty, “Development of a novel artifact-free eye shield based on silicon rubber-lead composition in the CT examination of the head,” *J. Radiol. Prot.*, vol. 39, no. 4, p. 991, 2019.
- [9]. A. Syakur and H. Sutanto, “Determination of hydrophobic contact angle of epoxy resin compound silicon rubber and silica,” in *IOP Conference Series: Materials Science and Engineering*, 2017, vol. 190, no. 1, p. 12025.
- [10]. M. D’Arienzo et al., “Gamma camera calibration and validation for quantitative SPECT imaging with ¹⁷⁷Lu,” *Appl. Radiat. Isot.*, vol. 112, pp. 156–164, 2016.
- [11]. Genç, D.T., Kovan, B., Demir, B. and Türkmen, C., 2019. Quality Control Tests of SPECT-CT. Süleyman Demirel University Faculty of Arts and Science Journal of Science, 14(1), pp.39-56.
- [12]. Hidayatullah, N., Sutanto, H., Anam, C., Wardhana, Y.W., Amilia, R., Naufal, A. and Taufiq, U.A., 2023. Evaluation of Elasticity, Dose Reduction, and Image Quality on Sr-Pb Shield for Thoracic CT Examination.
- [13]. Hirtl, A., Bergmann, H., Knäusl, B., Beyer, T., Figl, M. and Hummel, J., 2017. fully-automated analysis of Jaszczak phantom measurements as part of routine SPECT quality control. *Medical Physics*, 44(5), pp.1638-1645.
- [14]. Zanzonico, P. (2008). Routine quality control of clinical nuclear medicine instrumentation: a brief review. *Journal of Nuclear Medicine*, 49(7), 1114-1131.
- [15]. Busemann-Sokole, E. (2003). IAEA quality control atlas for scintillation camera systems.

Cite this article as :

Zaenal Arifin, Heri Sutanto, Siti Fairus, Anis Suhana , "Study of Phantom Images with Silicone Rubber on Single Photon Emission Computed Tomography (SPECT)", *International Journal of Scientific Research in Science and Technology (IJSRST)*, Online ISSN : 2395-602X, Print ISSN : 2395-6011, Volume 11 Issue 1, pp. 167-172, January-February 2024. Available at doi : <https://doi.org/10.32628/IJSRST52411116>
 Journal URL : <https://ijsrst.com/IJSRST52411116>